

ON DETECTING THE X-RAY SILHOUETTE OF A DAMPED LY $\alpha$  SYSTEM

MARK DIJKSTRA, ZOLTÁN HAIMAN &amp; CALEB SCHARF

Department of Astronomy, Columbia University, 550 West 120th Street, New York, NY 10027

Submitted to ApJ

## ABSTRACT

We explore the possibility of resolving an image of a damped Ly $\alpha$  (DLA) system in absorption against an extended, diffuse background X-ray source. Typical columns of neutral hydrogen in DLA systems are high enough to block out up to  $\sim 30\%$  of the soft X-ray flux at an observed photon energy of 0.5 keV, and we find that  $\sim 1\%$  of the area of extended X-ray sources at  $z \gtrsim 1$  have their 0.5 keV flux reduced by at least 20% because of intervening DLA systems. We discuss the observability of such absorption and find that  $\gtrsim 300$  photons per angular resolution element are required in the 0.3–8 keV band for its detection, and in order to distinguish it from intrinsic surface brightness fluctuations. For the surface brightness of the currently known high-redshift extended X-ray sources, this requires an integration time of a few Msec on *Chandra* if the maps are smoothed spatially to  $\approx 2''$  resolution. The exact required integration time depends on the DLA system's column density, metallicity and most strongly, its redshift. Current X-ray telescopes are likely to detect DLA systems with  $N_{\text{HI}} < 10^{22} \text{ cm}^{-2}$  only out to  $z \approx 2.3$ . The availability of DLA systems with a suitably high column-density for a silhouette detection is currently poorly known. We suggest that at low redshifts, archival data of bright X-ray point sources may be useful in constraining the high- $N_{\text{HI}}$  end of the column density distribution. We briefly discuss an alternative strategy of searching for extended X-ray sources behind known DLA systems. Although with current X-ray telescopes the detections are challenging, they will be within the reach of a routine observation with a next generation X-ray telescope such as the *X-Ray Evolving Universe Spectrometer* (*XEUS*) or *Generation-X*, and will deliver novel constraints on the nature of proto-galaxies.

*Subject headings:* cosmology: theory – galaxies: formation – galaxies: high-redshift – quasars: absorption lines – X-rays: galaxies

## 1. INTRODUCTION

Damped Ly $\alpha$  (DLA) absorbers owe their name to the presence of broad damping wings in their absorption profiles caused by column densities of neutral hydrogen in the range  $N_{\text{HI}} \sim 10^{20}$  to  $5 \times 10^{21} \text{ cm}^{-2}$ . These high column densities are only found in the cold disks of late-type galaxies in the local universe, but to identify the galaxies hosting this gas at cosmological redshifts has proven difficult, because of the overwhelming brightness of the background quasar in the optical. Only a dozen probable hosts for DLA systems at  $z \lesssim 1$  have been identified and their morphologies span a wide range (Chen & Lanzetta 2003; Rao et al. 2003).

So far several hundred DLA systems have been found in optical and ultraviolet quasar absorption spectra in the redshift range  $z \sim 0.1 – 4.6$  (Curran et al. 2002). It has been shown that at  $z \gtrsim 3$  they are the main contributors to  $\Omega_{\text{HI}}$  (Rao & Turnshek 2000; Storrie-Lombardi & Wolfe 2000; Prochaska & Herbert-Fort 2004), and make up the largest reservoir of cold gas available for starformation. Indeed,  $\Omega_{\text{HI}}$  at  $z \approx 3$  is comparable to  $\Omega_*$  at  $z \approx 0$ , the cosmic mass density of stars in the local universe (Wolfe et al. 1995).

It has therefore been argued that DLA systems are the progenitors of present-day galaxies. The exact nature of these progenitors however, is controversial: some have argued that DLA systems are large proto-galactic disks, based on (1) the asymmetric profiles of the low-ionization absorption lines, which are explained if the metals are present in a large, rapidly rotating disk (Prochaska & Wolfe 1997) and (2) the large ( $R > 15 – 30$  kpc; -e.g., Chen & Lanzetta 2003, Chen 2005) physical separation between the absorber and possible associated starlight in a few cases. Others have argued that these data are consistent with DLA systems being a collection of much smaller ( $\lesssim 5$  kpc) compact HI clouds falling onto a galaxy in their vicinity

(Maller et al. 2001; Haehnelt et al. 1998) and that these models provide a better fit to the kinematic data on the high ionization gas (Maller et al. 2003). The collection of clumps in this scenario extends over an angular scale comparable to that of the single large disk. A distinguishing feature between the models is therefore the smoothness of the DLA system's gas.

Determining the nature of the progenitors of our present-day galaxies is an important step in understanding galaxy formation in general. Obtaining a spatially resolved image of the neutral gas in a DLA system will be an important step in settling this issue. Unfortunately, detecting the neutral hydrogen in DLA systems in emission at  $z \gtrsim 0.5$  using the 21cm line on an existing telescope such as the Giant Metre-wave Radio Telescope (GMRT) is not feasible (e.g. Bagla 1999). Among planned future radio telescopes, only the Square Kilometer Array (SKA) has the appropriate sensitivity and frequency range to make such observations.

A major hindrance for constraining the properties of the DLA system's gas is the point-like character of the background quasars. Finding DLA systems in absorption against extended background sources would provide valuable additional information. In one example, Briggs et al. (1989) found that the dimensions of a disk-like absorber at  $z = 2$  are  $> 11$  kpc against an extended background radio source; ruling out compact gas configurations such as dwarf galaxies. In another case, Kanekar & Briggs (2003) have found HI 21cm absorption in a gravitational lens system at  $z = 0.76$  toward a quasar, from which the column density of hydrogen in the lens was estimated to be  $(2.6 \pm 0.3) \times 10^{21} \text{ cm}^{-2}$ . The lens is therefore a DLA system, but because the largest separation between a pair of radio images was small,  $\sim 0.7''$ , the gas configuration and extent could not be constrained. Fynbo et al. (1999) detected extended Ly $\alpha$  emission from a DLA system, that is illuminated by two nearby ( $\Delta z \lesssim 0.01$ ) quasars, and found the emission to extend over a region of

$3'' \times 6''$ . A disadvantage of this technique is that it only works when a bright source of ionizing radiation is physically very close to the DLA system.

In this paper, we examine the complementary possibility of detecting DLA systems against an extended background source emitting X-rays. The motivation for this approach is the discovery of the extended X-ray source 4C 41.17 by Scharf et al. (2003) at  $z = 3.8$ , with diffuse emission extending over  $\sim 100$  arcsec $^2$ . The X-ray spectrum is non-thermal and has a power-law index consistent with that of radio synchrotron emission. Scharf et al. (2003) conclude that the X-rays are most likely inverse Compton scattered cosmic microwave background(CMB) or far-infrared background photons. A similar source, 3C 294, was found by Fabian et al. (2003) at  $z = 1.8$  with diffuse emission extending over  $\sim 200$  arcsec $^2$ .

A silhouette of a galaxy containing neutral hydrogen against a background X-ray cluster has already been found at low redshift ( $z = 0.02$ , Clarke et al. 2004) and encourages us to explore diffuse X-ray sources as possible background screens against which to image DLA systems. Bechtold et al. (2001) found strong evidence for X-ray absorption in the direction of a  $z = 0.3$  DLA system in the spectrum of a  $z = 1.1$  quasar, a bright X-ray point source with one faint jet (Siemiginowska et al. 2002).

The outline of the rest of this paper is as follows. In §2, we introduce the X-ray optical depth through a DLA system and calculate the fraction of the sky covered by DLA systems as a function of their value of this optical depth. In §3, we describe how absorption by a DLA system can theoretically be distinguished from intrinsic surface brightness fluctuations and calculate the required integration times on *Chandra* to do this observationally. In §4, we discuss various contaminants that could mimick absorption by a DLA system; we also address the most important model uncertainties. The “inverse method” of searching for X-ray emission behind known DLA systems is discussed in §5. Finally, in §6, we present our conclusions and summarize the implications of this work.

Throughout this paper, we focus on an observed photon energy of  $E = 0.5$  keV. This choice reflects the fact that the absorption signature is strongest in the range  $E \sim 0.3 - 0.6$  keV (see §3), and that X-ray detectors are significantly less efficient at lower energies. We adopt the background cosmological parameters  $\Omega_m = 0.27$ ,  $\Omega_\Lambda = 0.73$ , and  $h = 0.71$  (Spergel et al. 2003).

## 2. SILHOUETTES OF DLA SYSTEMS

### 2.1. The X-Ray Optical Depth $\tau_{0.5}$ .

Typical neutral hydrogen column densities in DLA systems are in the range  $N_{\text{HI}} \sim 10^{20}$  to  $5 \times 10^{21}$  cm $^{-2}$  and are large enough to block a non-negligible fraction of X-rays emitted by sources that lie behind them. The optical depth through a column  $N_{\text{HI}}$  of hydrogen atoms for a photon of energy  $E$  is  $\tau(E) \sim 0.43 (N_{\text{HI}}/10^{21})(E/0.5 \text{ keV})^{-3.2}$ , for a gas that consists solely of a cosmic mix of 76% neutral hydrogen and 24% helium by mass. Observations indicate that the mean metallicity of DLA systems is  $\sim 10\%$  of the solar value with a modest redshift evolution (Prochaska et al. 2003). The presence of metals increases the optical depth. For example, the cross section per hydrogen atom in a gas with metallicity  $Z = 0.1Z_\odot$  is  $\sim 1.2(E/0.5 \text{ keV})^{0.3}$  times larger than in a metal free gas (e.g. Wilms et al. 2000). This shows that DLAs can show up in absorption against bright background X-ray sources (as detected already for a point-source by Bechtold et al. 2001).

We define the parameter  $\tau_{0.5}$  as the optical depth through

the DLA system at the photon energy  $E = 0.5$  keV in the observer’s frame,  $\tau_{0.5} \equiv N_{\text{HI}}\sigma_{\text{tot}}(0.5(1+z) \text{ keV})$ , where  $z$  and  $N_{\text{HI}}$  are the redshift and column density of neutral hydrogen atoms in the DLA system, respectively, and  $\sigma_{\text{tot}}(E)$  is the total absorption cross-section per hydrogen atom. This cross-section includes absorption by helium and heavier elements. To calculate  $\sigma_{\text{tot}}(E)$  of the DLA gas, we use the model described by Wilms et al. (2000). This model includes up-to-date photoionization cross sections and heavy elements in a solar abundance pattern, as well as H<sub>2</sub> molecules. We note that X-ray absorption arises predominantly from inner shells ionizations of metals, and ionization corrections are only important at gas temperatures much higher than those expected to occur in DLA systems.

### 2.2. The Influence of DLA Metallicity on $\sigma_{\text{tot}}$ and $\tau_{0.5}$ .

We consider the specific class of DLA systems with  $\tau_{0.5} = 0.1$ . Given  $\sigma_{\text{tot}}(E)$  and requiring  $N_{\text{HI}}\sigma_{\text{tot}}(E = 0.5(1+z) \text{ keV}) = \tau_{0.5}$ , we obtain a column density of hydrogen  $N_{\text{HI}}(z)$  for these DLA systems. In Figure 1, we show  $N_{\text{HI}}(z)$  as a function of redshift.

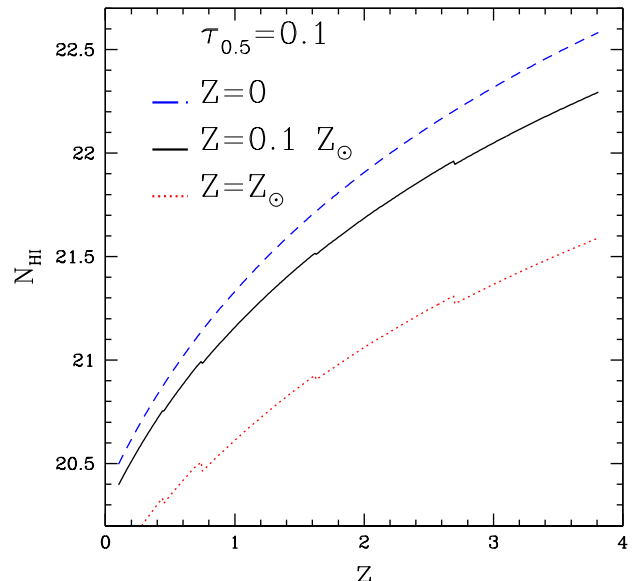


FIG. 1.— Column density of hydrogen required to produce an absorption optical depth of  $\tau_{0.5} = 0.1$  for photons with observed energy  $E = 0.5$  keV, as a function of redshift for three metallicities. To illustrate the importance of metallicity in DLA systems, we show three cases: DLA systems with no metals (dashed-blue line), with  $Z = Z_\odot$  (dotted-red line) and  $Z = 0.1Z_\odot$  (solid-black line). The last is our fiducial model. The highest observed column of neutral hydrogen among known DLA systems is  $\log(N_{\text{HI}}/\text{cm}^{-2}) = 21.7$  (Curran et al. 2002).

To illustrate the importance of the assumed metallicity, we show three cases:  $Z = 0$  (dashed-blue line),  $Z = Z_\odot$  (dotted-red line), and  $Z = 0.1Z_\odot$  (solid-black line). The last is our fiducial model, based on the mean observed metallicity. Note that the column of hydrogen required to produce a certain value of  $\tau_{0.5}$  can vary by an order of magnitude depending on the metallicity of the gas. The reason  $N_{\text{HI}}$  drops slightly but suddenly at  $z \sim 0.4, 0.7, 1.6, \dots$  is that  $E = 0.5(1+z)$  keV at these redshifts equals the K-shell ionization energy of one of the heavy elements and  $\sigma_{\text{tot}}$  ‘jumps’ to a larger value. For any other value of  $\tau_{0.5}$ , the corresponding column can be obtained by multiplying the value taken from Figure 1 by  $\tau_{0.5}/0.1$ . We find that the following formula provides an accurate fit to the relation between  $N_{\text{HI}}$ ,  $z$ ,  $Z$  and  $\tau_{0.5}$  for a DLA system:

$$\tau_{0.5} = 0.014 A(Z) \left( \frac{N_{\text{HI}}}{10^{21} \text{ cm}^{-2}} \right) \left[ \frac{0.5(1+z)}{1.5} \right]^{-3.2+B(Z)}, \quad (1)$$

where  $A(Z) = 1.0 + 5.39Z$ , and  $B(Z) = 0.64 \arctan[(Z/0.19)^{0.91}]$

This formula is good to within 5% for  $Z < 0.1Z_{\odot}$ , and to within 10% for  $Z < Z_{\odot}$ . The main reason for the deteriorating accuracy of the fitting formula at larger metallicities, is that the ‘jumps’, in the absorption cross-section are more pronounced in these cases. It is exactly at these jumps that the fit is worse.

### 2.3. The Covering Factor of DLAs.

In §2.2 we calculated the column of hydrogen in a DLA system required to produce a given value of the X-ray optical depth  $\tau_{0.5}$  as a function of its redshift. In this section we calculate what fraction of the sky is covered by DLA systems with various minimum values of  $\tau_{0.5}$ .

The total number of DLA systems along a single line of sight (LOS) with  $\tau_{0.5}$  or larger between redshift 0 and  $z_s$ , where  $z_s$  is the redshift of a hypothetical extended background source, is given by:

$$\mathcal{N} = \int_0^{z_s} dz \int_{N_{\text{HI}}(z)}^{\infty} dN_{\text{HI}} f(N_{\text{HI}}, z), \quad (2)$$

where  $N_{\text{HI}}(z)$  is the column of hydrogen corresponding to  $\tau_{0.5}$  and  $f(N_{\text{HI}}, z) dN_{\text{HI}} dz$  is the number of DLA systems in the range  $N_{\text{HI}} \pm dN_{\text{HI}}/2$  and  $z \pm dz/2$ . We adopt  $f(N_{\text{HI}}, z)$  from Péroux et al. (2003, hereafter P03), who find that the data can be best fitted with a  $\Gamma$  function used in studies of the galaxy luminosity function.<sup>1</sup> Note that  $\mathcal{N}$  can equivalently be interpreted as the two-dimensional covering factor of these DLA systems;  $f_{\text{cov}} \equiv \mathcal{N}$ . The exact form of  $f(N_{\text{HI}}, z)$  is an important uncertainty in our model. The total sample of DLAs is still too small to constrain  $f(N_{\text{HI}}, z)$  well, especially at the low redshifts and high-column densities that are most important for our purposes. We discuss this uncertainty in more detail in §4.2 below.

In Figure 2, we plot  $f_{\text{cov}}$  as a function of  $\tau_{0.5}$ , with the X-ray source located at  $z_s = 3.8$  (motivated by the source found by Scharf et al. 2003, 4C 41.17). The three thin curves represent the same three cases shown in Figure 1 in which the DLA gas has no metals (dashed-blue line),  $Z = 0.1Z_{\odot}$  (solid-black line) and  $Z = Z_{\odot}$  (dotted-red line). The covering factor increases with metallicity because the column of hydrogen required to produce a certain value of  $\tau_{0.5}$  decreases with increasing metallicity. (The thick solid line addresses a scatter in metallicities, as explained in §2.4 below.)

Figure 2 shows for example, that for the fiducial model ( $Z = 0.1Z_{\odot}$ ) a fraction  $f_{\text{cov}} \sim 0.03$  and 0.01 of the sky is covered by DLA systems that absorb at least  $\sim 10\%$  and  $\sim 20\%$ , respectively, of the 0.5 keV photons from the background object. For different energies,  $\tau_E \sim \tau_{0.5} \times [\sigma_{\text{tot}}(E)/\sigma_{\text{tot}}(0.5 \text{ keV})]$ , since the absorption cross-section is close to a pure power-law.

The main conclusion from Figure 2 is that for a source similar to 4C 41.17, which has a size of  $\sim 100 \text{ arcsec}^2$ , observed at  $\sim \text{arcsecond}$  resolution, one can hope to find several pixels covered by DLA systems with opacities up to  $\tau_{0.5} \sim 0.1 - 0.2$ . Of course, for a source covering a larger solid angle and/or in

<sup>1</sup>Note that we obtain  $f(N_{\text{HI}}, z)$  by multiplying the functions quoted in P03 by  $dX(z)/dz$ . Their function describes the number of DLA systems in the range  $X(z) \pm dX(z)/2$ , where  $dX(z)/dz \equiv (1+z)^2 (H_0/H(z))$  is the absorption distance, originally introduced by Bahcall & Peebles (1969), where  $H_0$  and  $H(z)$  are the Hubble parameters at redshift 0 and  $z$ , respectively.

the case of an unusually metal-enriched DLA system, there is a significant probability of finding more opaque absorption. For example, in the case of an X-ray emitting galaxy cluster with  $\sim 10$  times the area of 4C 41.17 (see below), the figure shows that DLA systems with  $\tau_{0.5} \gtrsim 0.3$  should typically obscure several pixels.

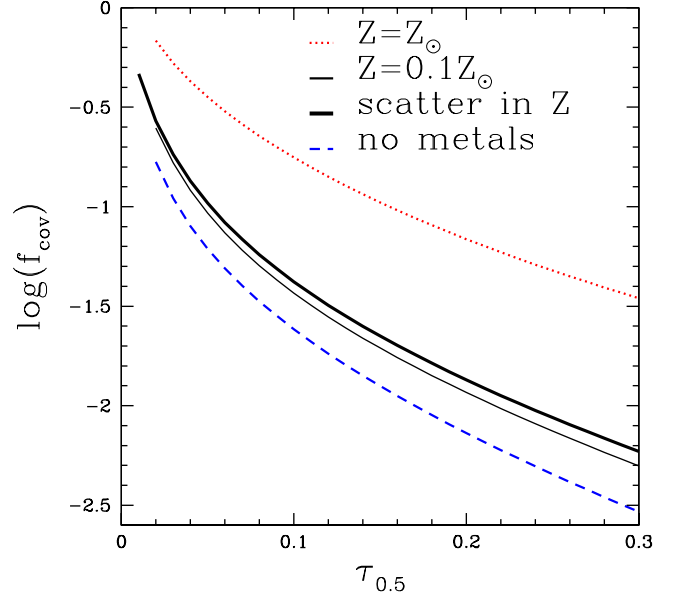


FIG. 2.— Covering factor  $f_{\text{cov}}$  on the sky of DLA systems between  $z = 0$  and  $z_s = 3.8$  that have an X-ray optical depth  $\tau_{0.5}$  or larger, plotted as a function of  $\tau_{0.5}$ . The three curves represent the same three metallicities as in Figure 1. The thick, solid line represents an alternative model, discussed in §2.4, in which the DLA systems have a log-normal distribution with mean  $\log(Z/Z_{\odot}) = -1.0$  and  $\sigma_{\log Z/Z_{\odot}} = 0.5$ .

### 2.4. Uncertainties in $f_{\text{cov}}$ .

The calculation of  $f_{\text{cov}}$  has two main uncertainties. They are discussed here.

The larger of the two uncertainties is associated with the function  $f(N_{\text{HI}}, z)$ . The redshift of the source,  $z_s$ , has only a small effect on the results for  $\tau_{0.5} \gtrsim 0.1$ . The reason is that with the  $f(N_{\text{HI}}, z)$  adopted from P03, the absorption is dominated by low redshift systems; e.g. 75% of the contribution to  $f_{\text{cov}}$  comes from  $z < 0.61$  and the contribution from sources with  $z \gtrsim 1.4$  is practically negligible. This inference, however, depends sensitively on the poorly known redshift-evolution of  $f(N_{\text{HI}}, z)$ , and the contribution to  $f_{\text{cov}}$  from high- $z$  systems may be much larger (discussed further in §4.2).

The second uncertainty involves the metallicity of the DLA gas. Figure 2 shows that the covering factor depends quite strongly on the assumed metallicity. Our fiducial model assumes  $Z = 0.1Z_{\odot}$ , based on the mean observed value. There is however, considerable scatter in  $Z$  around this mean; the metallicity can easily vary by an order of magnitude between individual objects (Prochaska et al. 2003). Since enhanced metallicity increases  $f_{\text{cov}}$  more than reduced metallicity decreases it, one may expect that incorporating the scatter enhances  $f_{\text{cov}}$ .

We quantified in an alternative model the effect of this observed scatter in metallicities on  $f_{\text{cov}}$ . A log-normal distribution of metallicities around the mean  $\log(Z_{\text{DLA}}/Z_{\odot}) = -1.0$  with a standard deviation of  $\sigma_{\log(Z_{\text{DLA}}/Z_{\odot})} = 0.5$  was assumed (we imposed a maximum value of  $Z = Z_{\odot}$  since larger metallicities

have never been observed Prochaska et al. 2003). In this model  $\lesssim 10\%$  of the DLA systems have metallicities  $\log(Z_{\text{DLA}}/Z_{\odot}) < -1.6$  and  $> -0.4$ . Our results for this alternative model are shown by the thick solid line in Figure 2. We find that the scatter causes a net small increase in  $f_{\text{cov}}$ , as expected, but that in the entire range in  $\tau_{0.5}$  plotted, the increase is  $\lesssim 25\%$ , which is well within the other model uncertainty mentioned above.

### 3. OBSERVABILITY

The ideal background source against which to detect a DLA system is a bright and perfectly smooth extended X-ray source. In this idealized case a foreground DLA system (or that part of the DLA that intersects the extended X-ray source) shows up in absorption against the background source in the very soft X-ray band (0.3–0.6 keV). In practice, extended X-ray sources are not smooth, but have surface brightness fluctuations that are much larger than the  $\sim 10\%$  level introduced by absorption because of intervening DLA systems. For example, the fluctuations in the number of X-ray photons received from different locations in 4C 41.17 exceeds roughly 100%. The main reason for this is small number statistics. The mean number of counts per pixel is  $\sim$  a few, and therefore Poisson noise will make variations between individual pixels large. In 3C 294 (Fabian et al. 2003), the mean number of counts per pixel is higher by a factor of a few and therefore Poisson noise is less severe, although it is still large enough to introduce errors well in excess of 10%. Large holes in the X-ray map of 3C 294 are clearly seen, from which no X-rays at all are detected, and which are too large to arise from an intervening absorber. They probably arise from intrinsic spatial variations in the population of relativistic particles responsible for the scattering. We next describe two methods to distinguish the intrinsic surface brightness fluctuations from those caused by absorption.

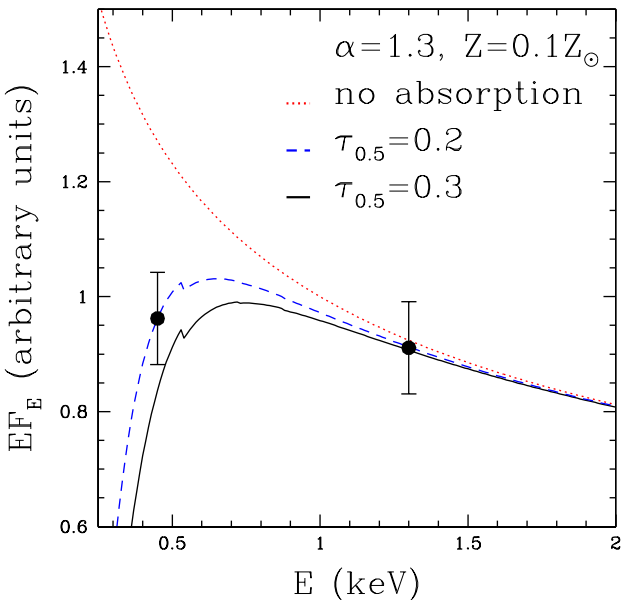


FIG. 3.— Power-law spectrum,  $F_E \propto E^{-1.3}$  of an unobscured (dotted-red line), and an obscured X-ray source. The X-ray source is obscured by a column of hydrogen corresponding to  $\tau_{0.5} = 0.2$  (dashed-blue) and  $\tau_{0.5} = 0.3$  (solid-black). In Figure 1 the required column of hydrogen to produce  $\tau_{0.5} = 0.1$  can be read off as a function of  $z$ . The two mock data points show the error on the spectrum if such a source were observed and its spectrum binned in three energy bands: 0.3–0.6, 0.6–2.0 and 2.0–8.0 keV, assuming the total number of photons received in the energy range 0.3–8.0 keV is 300 (see text).

### 3.1. Spectral Imprints of DLA Systems

Because the absorption cross section is a strong function of energy ( $\sigma_{\text{tot}} \propto E^{-3}$ ), the spectrum of an attenuated portion of the extended X-ray source can, in principle, reveal whether X-rays have been absorbed by an intervening column of gas. In order to make a crude estimate of the sensitivity of X-ray observations to DLA attenuation, we here quantify the absorption signature in a simple toy-model. In reality, an X-ray observatory has a potentially complex, energy dependent, detection efficiency, which must be taken into account in a more detailed analysis (more discussion on this is deferred to §3.1.1).

In Figure 3, we show the spectrum of an unobscured X-ray source with a power law spectrum  $F_E \propto E^{-\alpha}$  with  $\alpha = 1.3$  (dotted-red line, motivated by the inverse Compton spectrum observed in 4C 41.17). The units of the flux are arbitrary. Also shown is the spectrum of the same source, obscured by an intervening column of hydrogen with  $\tau_{0.5} = 0.2$  (dashed-blue line) and  $\tau_{0.5} = 0.3$  (solid black line). In these cases, absorption has removed  $\sim 18\%$  and  $\sim 26\%$  of the 0.5 keV photons, respectively. The two mock data points with errorbars are discussed in §3.1.1. Clearly, the spectra are most distinct at energies  $E \lesssim 0.6$  keV.

Unfortunately, the unobscured case is purely hypothetical since omnipresent Galactic HI will always absorb a small amount of X-rays. The X-ray optical depth through the Galaxy  $\tau_{\text{Gal}}$  is typically 0.2, although there are large parts of the sky in which it is less than that by a factor of a few. Spatial variations in the total column of Galactic hydrogen across angular scales comparable to the sizes of known extended X-ray sources are negligible. Therefore galactic HI will obscure the entire X-ray source by the same known amount and effectively steepen its spectrum at low energies (see §4.1). To find an absorption signature of a  $\tau_{0.5} = 0.1$  DLA system, for example, we therefore need to distinguish between the  $\tau_{\text{Gal}} = 0.2$  and  $\tau_{\text{Gal}} + \tau_{0.5} = 0.3$  cases (which are both shown in Fig. 3).

In practice, for any source, one would proceed by first determining the mean *observed* spectrum of the entire extended X-ray source. This mean spectrum can then be used as a template, to seek differential spectral deviations in spatial bins along the surface of the source.

To quantify the difference in the spectra, we introduce the ratio  $\mathcal{R}$ , which is the ratio of the number of photons received in the very soft (0.3–0.6 keV) and the soft (0.6–2.0 keV) band. In Figure 4, we plot  $\mathcal{R}$  in the case of no absorption for a power law  $F_E \propto E^{-\alpha}$  spectrum as a function of  $\alpha$  together with  $\mathcal{R}$  for cases in which  $\tau_{0.5} = 0.2, 0.3$  and  $0.4$ . Note that the case  $\tau_{0.5} = 0$  (dotted-red line) is hypothetical, but shown for completeness. The case  $\tau_{0.5} = 0.2$  (dashed-blue line) illustrates the case in which there is Galactic absorption only, whereas the cases  $\tau_{0.5} = 0.3$  (solid-black line) and  $0.4$  (long-dashed-green line) correspond to cases in which there is additional absorption from a DLA system with  $\tau_{0.5} = 0.1$  and  $0.2$ .

Figure 4 shows, for example, that for  $\alpha = 1.3$  and  $\tau_{0.5} = 0$ ,  $\mathcal{R} = 1.8$  decreases to  $\sim 1.2/1.1$  and  $0.9$  for  $\tau_{0.5} = 0.2/0.3$  and  $0.4$ , respectively. There is, of course, a degeneracy with  $\alpha$ ; for example,  $\mathcal{R}$  can also equal 0.9 with no additional DLA absorption when  $\alpha = 0.9$ . Two approaches to lift this degeneracy are: (1) determining  $\alpha$  via extrapolation from the  $E > 1.0$  part of the spectrum, and/or (2) computing  $\mathcal{R}$  as a function of position, which may reveal areas where  $\mathcal{R}$  is significantly lower than in the rest of the source. The latter approach is similar to mapping out dust using an optical map, with the difference that obscured

parts of the X-ray source look ‘bluer’, rather than redder.

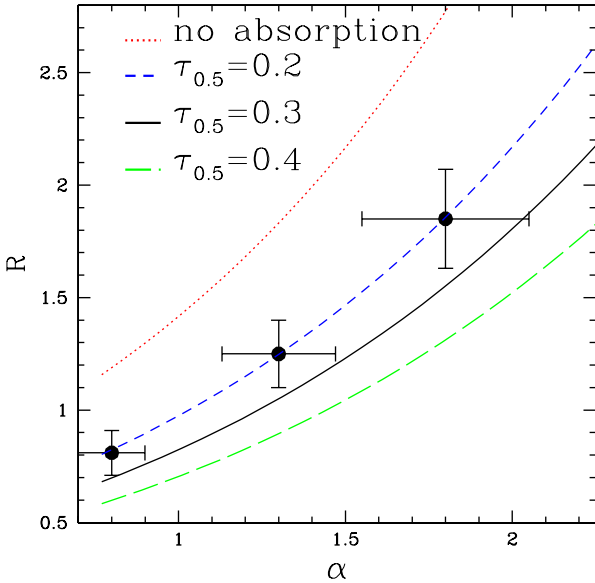


FIG. 4.— Ratio of the number of photons in the observed 0.3-0.6 keV and 0.6-2.0 keV bands, defined as  $\mathcal{R}$ , as a function of the slope of the spectrum  $\alpha$ . The different curves correspond to different amounts of absorption for a range of 0.5 keV optical depths of 0–0.4, as shown by the labels. The three mock data points denote the error on  $\mathcal{R}$  and  $\alpha$  for  $\alpha = 0.8, 1.3$ , and  $1.8$ , provided the total number of detected photons in the energy range  $0.3–8.0$  keV is  $300$ .

### 3.1.1. Photon Statistics

We next address the uncertainty in  $\alpha$  and  $\mathcal{R}$  given that we receive  $n_{\text{ph}}$  photons in the energy range  $0.3–8.0$  keV from a specific location on the sky. We bin the spectrum in the  $0.6–2.0$  and  $2.0–8.0$  keV bands to two data points from which we extract the slope of the spectrum,  $\alpha$ . The reason we only use these two bands is that they are not strongly affected by obscuration (see Fig. 3).

As an example, we consider the case  $\alpha = 1.3$ : the number of photons in the  $0.3–0.6$ ,  $0.6–2.0$  and  $2.0–8.0$  keV bands is  $149(n_{\text{ph}}/300)$ ,  $123(n_{\text{ph}}/300)$  and  $28(n_{\text{ph}}/300)$ , respectively for  $\tau_{0.5} = 0.2$ , which represents the case in which there is Galactic absorption only. The ratio of the number of photons in the  $0.6–2.0$  and  $2.0–8.0$  keV bands is set by  $\alpha$ . Assuming Poisson noise on the number of photons in each bin, we find the uncertainty in  $\alpha$  and  $\mathcal{R}$  to be,  $\sigma_\alpha \sim 0.2$  and  $\sigma_{\mathcal{R}} \sim 0.15$ . We repeated the calculation of the uncertainty for  $\alpha = 0.8$  and  $\alpha = 1.8$ . The results for  $\alpha = 0.8, 1.3$  and  $1.8$  are shown as three ‘data points’ in Figure 4. We find the following rough scaling relations of the errors:  $\sigma_\alpha \sim 0.17(\alpha/1.3)$  and  $\sigma_{\mathcal{R}} \sim 0.15(\alpha/1.3)^{1.2}$ . The  $\alpha$ -dependence of the errors reflect that as  $\alpha$  increases, the number of photons in the harder bands decreases, which makes the uncertainty there larger.

Figure 4 shows that the  $\tau_{0.5} = 0.3$  and  $0.4$  curves are separated by  $1$  and  $2\sigma$ , respectively, from the  $\tau_{0.5} = 0.2$  curve, with a weak dependence on  $\alpha$ . We write the level significance  $S$  at which absorption can be detected as:

$$S = 2\sigma \left( \frac{\tau_{0.5}}{0.2} \right) \left( \frac{n_{\text{ph}}}{300} \right)^{0.5} \left( \frac{1.3}{\alpha} \right)^{0.5} \quad (3)$$

The above estimates ignore the processing of the input signal through the X-ray instrument. The typical response function of

X-ray telescopes like *Chandra* are strong functions of energy. *Chandra* is a factor of  $\sim 1.5–2$  and  $\sim 3–4$  more sensitive at  $E = 1.0$  keV than it is at  $E = 0.5$  and  $0.3$  keV, respectively. In addition, *Chandra*’s sensitivity decreases roughly linearly for  $E \gtrsim 4.0$  keV. Since the response function is known, one can correct for this, leaving the values of  $\mathcal{R}$  we calculated unchanged. The errors, however, are affected by this response function. For a fixed number of detected photons in the energy range  $0.3–8.0$  keV from a source with a certain  $\alpha$ , we find that the total number of photons in the  $0.3–0.6$  and  $2.0–8.0$  keV bands is reduced by a factor of  $\sim (0.7–0.8)$  and  $\sim (0.8–1.0)$ , respectively, whereas it is increased by a factor of  $\sim 1.3–1.4$  in the  $0.6–2.0$  keV band. We find that this barely affects the errors on  $\mathcal{R}$  and  $\alpha$  and conclude that equation (3) remains unchanged by a proper treatment of the energy response function.

For comparison, Bechtold et al. (2001), detected  $198$  photons in the  $0.4–8.0$  keV energy band for a source with  $\alpha = 1.5 \pm 0.2$  in a  $3$  ks observation of Q1331+170 with *Chandra*. First we notice that the error on  $\alpha$  is the same as our estimate (note that  $198$  photons in the energy band  $0.4–8.0$  keV, corresponds to  $271$  photons in the band  $0.3–8.0$  keV for  $\alpha = 1.5$ ). With this number of photons, their non-detection puts an upper limit of  $\sim 10^{22}$  cm $^{-2}$  to the column of hydrogen for the DLA system along the LOS at  $z = 1.77$  at the  $3\sigma$  level. Assuming  $Z = 0.1Z_\odot$ , this can be translated to an upper limit to the value of  $\tau_{0.5}$  for the DLA system of  $0.26$ . If we interpret this upper limit of  $\tau_{\text{Gal}} + \tau_{0.5} = 0.46$  at the  $3–\sigma$  level as a statement that the separation between the  $\tau_{0.5} = 0.46$  and  $0.2$  curves is  $3\sigma$ , then this is also in good agreement with equation (3), which predicts  $S = 2.3\sigma$ . The numbers lie even closer together when we take into account that the value of  $\tau_{\text{Gal}}$  in the direction of Q1331+170 was actually  $0.12$  instead of  $0.2$ , confirming that our simple estimate is a good first-order approximation for the expected signal.

### 3.1.2. Required Integration Times on *Chandra*

In §3.1.1 we found that we need several hundred X-ray photons to have a  $2\sigma$  detection of a foreground DLA system along the LOS, with the exact number depending on the slope of the X-ray spectrum of the background source, and the value of  $\tau_{0.5}$  of the foreground DLA system. To make a map that spatially resolves a DLA system we need several hundred photons per pixel in the image.

Ideally, we also need surface brightness maps with arcsecond resolution to be able to differentiate between compact clumps ( $d \lesssim 5$  kpc) and large disks ( $R \gtrsim 15–30$  kpc, or  $D \gtrsim 30–60$  kpc, e.g. Chen 2005), since  $1''$  corresponds to  $\sim 7–8.5$  kpc in the redshift range  $0.7–4.0$ . To reduce telescope time, the maps can be binned to a resolution of  $2'' \times 2''$ . If the DLA gas resides in a large ( $D \gtrsim 30–60$  kpc) disk, it will be resolved in  $\gtrsim 5–16$  resolution elements.

To obtain  $\gtrsim 3 \times 10^2$  photons per resolution element, we need  $\gtrsim 75$  photons arcsec $^{-2}$ . We can express the required integration time for a detection in one resolution element (pixel) at significance level  $S$  as:

$$t_{\text{int}} = 3.0 \left( \frac{0.2}{\tau_{0.5}} \right)^2 \left( \frac{\alpha}{1.3} \right) \left( \frac{2.5 \times 10^{-5}}{\text{counts s}^{-1}} \right) \left( \frac{S}{2\sigma} \right)^2 \text{Ms} \quad (4)$$

$$= 3.0 \left( \frac{2.7 \times 10^{21}}{N_{\text{HI}}} \right)^2 \left( \frac{1+z}{2} \right)^{5.8} \left( \frac{\alpha}{1.3} \right) \left( \frac{2.5 \times 10^{-5}}{\text{ct/s}} \right) \left( \frac{S}{2\sigma} \right)^2 \text{Ms}, \quad (5)$$

where counts s $^{-1}$  is the count rate of the total number of photons in the energy band  $0.3–8.0$  keV per arcsec $^{-2}$ . To arrive at the second line (eq. 5), we assumed  $Z = 0.1Z_\odot$ , and used

equation (1) to eliminate  $\tau_{0.5}$ . The strong redshift dependence of the required integration time puts constraints on which subclasses of DLA systems can be detected in this manner. If 3 Ms is taken as an absolute upper limit on the total integration time, the minimum required column of hydrogen in the DLA system as a function of redshift is  $N_{\text{HI}} = 2.7 \times 10^{21} [(1+z)/2]^{2.9} \text{ cm}^{-2}$  in order for it to be detected. If we assume  $N_{\text{HI}}$  cannot exceed  $10^{22} \text{ cm}^{-2}$ , then the method fails to detect DLA systems at  $z > 2.30$ . Note that although the maximum observed  $\log(N_{\text{HI}}/\text{cm}^{-2}) = 21.7$ , theoretically there is no evidence for an upper limit at this value of  $N_{\text{HI}}$ . The numbers given above are all dependent on the assumed metallicity, on  $\alpha$  and on the brightness of the background X-ray source.

The quoted count rate of  $2.5 \times 10^{-5} \text{ counts s}^{-1}$  is motivated by the few recently observed high-redshift extended X-ray sources. For example, 4C 41.17 was observed for 100 ks on *Chandra* by Scharf et al. (2003) and has a few photons  $\text{arcsec}^{-2}$  over its  $\sim 100 \text{ arcsec}^2$  area. Another source, 3C 294, was observed for 200 ksec with *Chandra* and has  $\gtrsim 4\text{--}6$  photons per  $\text{arcsec}^2$  over most of its area of  $\sim 200 \text{ arcsec}^2$  (Fabian et al. 2003). Note that there are regions where the count rate is higher.

Grego et al. (2004) observed a distant ( $z = 0.8$ ) galaxy cluster for 100 ksec using *Chandra*. In their observation an area as large as  $\sim 10^3 \text{ arcsec}^2$  had more than 2.5 photons  $\text{arcsec}^{-2}$ . The origin of the X-rays in this case is mainly thermal, and the analysis given above for a power-law inverse Compton spectrum does not apply. However, a cluster X-ray spectrum in reality is more complex, with many heavy element emission lines superimposed on a multi-temperature thermal Bremsstrahlung spectrum (Raymond & Smith 1977). A power law with photon index of  $\alpha \approx 0.5\text{--}1$  can therefore be used as a simple first-order approximation, and similar statistics will apply. An advantage of using galaxy clusters (over the X-ray halos of radio galaxies) is their potentially larger angular size, which allows a search for the rarer DLA systems with more significant opacity.

### 3.2. Combining X-ray and Sunyaev-Zeldovich Effect Maps

Another way to determine whether a dimming of certain part(s) in the X-ray image is due to absorption or to an intrinsic brightness fluctuation in the source itself is to map the CMB temperature decrement, caused by the Sunyaev-Zeldovich (SZ) effect, along the surface of the source. This decrement should scale with the intrinsic X-ray brightness, regardless of whether the origin of the X-rays is thermal or non-thermal. In particular, thermal X-ray emission scales with the line-of-sight integral of  $n_e^2$ , whereas inverse Compton emission and the SZ surface brightness both scale with the LOS sight integral of  $n_e$  (where  $n_e$  is the electron number density). Local density variations can therefore cause thermal X-ray and SZ brightness variations. However, the thermal X-ray flux is unlikely to drop noticeably without an accompanying decrease in the SZ decrement. In contrast, an intervening DLA system would not have any effect on the SZ decrement. An SZ map with approximately arcsecond resolution would therefore be very useful in constraining the intrinsic X-ray brightness fluctuations. This resolution will be feasible with future millimeter telescopes, such as the *Atacama Large Millimeter Array* (ALMA)<sup>2</sup>. Whether ALMA is sensitive enough to detect SZ temperature decrements due to sources like 4C 41.17 can be estimated as follows: As a first order estimate, the temperature decrement at  $\nu \sim 100\text{--}200 \text{ GHz}$  can be approximated by  $\Delta T_{\text{CMB}} \sim (N_e T_e / 10^{28} \text{ K cm}^{-2})$

$\mu\text{K}$ , where  $N_e$  is the column density of electrons in the X-ray source,  $T_e = \bar{E}/k$  is the electron temperature, and  $\bar{E}$  is the mean electron energy. The product  $N_e T_e$  is directly proportional to the observed rate of X-ray photons,  $\dot{N}_\gamma$ , which is given by  $\dot{N}_\gamma = \epsilon dV / (4\pi d_L^2(z) d\Omega \bar{E}_\gamma)$  photons  $\text{cm}^{-2} \text{ s}^{-1} \text{ sr}^{-1}$ . Here  $\epsilon = 5.4 \times 10^{-36} T_e N_e (1+z)^4 \text{ ergs s}^{-1} \text{ cm}^{-3}$  is the volume emissivity from inverse Compton emission (e.g., Katz et al. 1996);  $d_L(z)$  is the luminosity distance;  $\bar{E}_\gamma$  is the mean observed photon energy, and  $dV$  and  $d\Omega$  are differential volume and solid angle elements, respectively. For 4C 41.17,  $\sim 2$  photons  $\text{arcsec}^{-2}$  are observed, implying  $N_e T_e \sim 10^{30}$  in the above units. Therefore, we find  $\Delta T_{\text{CMB}} \sim 10^2 \mu\text{K}$ , which can be detected by ALMA within several hours of integration (Kocsis et al. 2005).

## 4. DISCUSSION

### 4.1. The Absorber's Location along the LOS

We found that it is possible to detect DLA systems in absorption against background X-ray sources, but generally the redshift of the absorber along the LOS is not constrained (except in the rare cases in which the absorption signature is very strong; Bechtold et al. 2001). In this section we discuss possible contaminants that could leave an absorption feature similar to a DLA system along a random position along the LOS. The sequence in which the contaminants are discussed is based on their distance to us. We start with Galactic HI and end with neutral gas physically associated with the source.

Galactic HI is present in large columns; the average column of hydrogen within our own Galaxy is  $\langle N_{\text{HI}} \sin|b| \rangle = 3 \times 10^{20} \text{ cm}^{-2}$ , where  $b$  is Galactic latitude and  $\langle \dots \rangle$  denotes the average over an annulus at  $b$  (Lockman e.g., 2003). Assuming a solar abundance pattern of  $Z = 0.7 Z_\odot$  (which is the appropriate value for the interstellar medium (ISM), e.g. Wilms et al. 2000) for this column, this translates to  $\langle \tau_{\text{Gal}} \sin|b| \rangle = 0.19$ . Because of spatial variations of Galactic  $N_{\text{HI}}$ , there are large portions of the sky where  $\tau_{\text{Gal}}$  is lower by a factor of a few. These spatial variations occur predominantly on large ( $> 1^\circ$ ) angular scales, and therefore  $\tau_{\text{Gal}}$  can be considered as a constant over the entire X-ray source. The rms spatial fractional variation in Galactic  $N_{\text{HI}}$  is  $< 3\%$  on angular scales  $< 1^\circ$ , with larger fluctuations occurring on smaller angular scales only in directions of anomalously high Galactic  $N_{\text{HI}}$  (Lockman 2003). This leads to the conclusion that the Galactic column can be treated as constant across the extended X-ray source, and is unlikely to present a problem beyond changing the effective slope of the X-ray source at low ( $E < 0.6 \text{ keV}$ ) energies.

The regions of anomalously high  $N_{\text{HI}}$  are not found only in the Galactic plane, but clusters of HI clouds associated with the galaxy are found at Galactic latitudes  $> 10\text{--}20^\circ$  (Lockman & Pidopryhora 2004). The association of this gas with the galaxy is clear because its kinematics closely matches that of the planar gas. Less clear is this association for the High Velocity Clouds, which have velocities that deviate by  $> 50 \text{ km/s}$  (Wakker & van Woerden 1997) from the allowed range based on a model of Galactic rotation. The nature of these HVCs is not well understood, mainly because the distance to them is observationally poorly constrained. Possible contamination by HVCs or extraplanar galactic clouds can be avoided simply by avoiding the directions in which they are detected, as mentioned earlier. However, potentially smaller versions of HVCs or any kind of extraplanar HI cloud may contaminate our signal.

A small compact HI cloud with an angular size of  $\sim 5''$  and a column of a few times  $10^{20} \text{ cm}^{-2}$  would go undetected in cur-

<sup>2</sup>See <http://www.alma.nrao.edu/>

rent HI observations, and could mimic the absorption signature of a DLA system at a cosmological distance. We discuss below why these clouds, if they somehow manage to form, are probably short-lived and probably not a contaminant we should worry about. For a cloud with  $N_{\text{HI}} = 3 \times 10^{20} \text{ cm}^{-2}$  at a distance  $D = 100 \text{ kpc}$  with an angular size of  $\theta = 5 \text{ arcsec}$ , we obtain an HI mass of  $\sim 10(D/100 \text{ kpc})^2 (\theta/5'')^2 M_{\odot}$  compressed in a cloud of radius  $1.2(D/100 \text{ kpc}) (\theta/5'') \text{ pc}$ . With a mean number density of  $\sim 2.5 \times 10^2(d/10 \text{ Mpc})^{-1} (\theta/5'')^{-1} \text{ cm}^{-3}$  these clouds are only self-gravitating if the temperature inside them is  $\sim 4(D/100 \text{ kpc}) \text{ K}$ . These cold, high density environments are typical for molecular clouds (although these are more massive, with  $M \sim 10^5 M_{\odot}$ ). Therefore one would expect these clouds to be sites of starformation as well, in which one cloud would form only a few stars (or one star) on a short timescale. Note that if these clouds were truly isolated, another threat to their stability would be thermal contact with a hot surrounding medium (the Galactic halo gas or the intergalactic medium). Heat conduction would rapidly raise the cloud's temperature, which would cause it to expand and lower its column density.

The required columns are also typically reached in cold disks of late-type galaxies in the nearby universe, which would be bright and easy to identify in optical images. Furthermore, even if the HI is associated with faint galaxies, it will be easier to identify than in the case of DLAs discovered in optical quasar spectra, because there would be no bright background quasar dominating the optical images.

Another possibility is that the hydrogen gas is physically associated with the source. Whether a significant amount of neutral hydrogen can co-exist with the hot, X-ray emitting gas should depend primarily on the local cooling efficiency. In recent work, Birnboim & Dekel (2003) and Keres et al. (2004) have argued that significant neutral gas is present only around low-mass, high-redshift galaxies. Sources that are sufficiently X-ray bright to allow the detection of a DLA system are likely to be associated with more massive objects (such as powerful radio galaxies), in which the local neutral hydrogen would be absent. In any case, absorption in a region that is several arcseconds across would imply that the neutral hydrogen gas associated with the source itself would extend several tens of kiloparsecs across, which would be an interesting alternative interpretation of any future detection.

We conclude that the two contaminants that cannot be ruled out observationally, the compact, cold, Galactic clouds or mini HVCs and the HI associated with the X-ray source, both offer interesting alternative interpretations of any future detection.

#### 4.2. The Uncertainties in $f(N_{\text{HI}}, z)$

As mentioned above, an important uncertainty in our predictions is the poorly known column-density distribution  $f(N_{\text{HI}}, z)$  at low redshifts and high columns. The total number of DLA systems used by P03 to constrain  $f(N_{\text{HI}}, z)$  in the DLA range of  $N_{\text{HI}}$  was 114. These data were binned into four redshifts bins covering the redshift ranges  $z = 0.0 - 2.0$ ,  $2.0 - 2.7$ ,  $2.7 - 3.5$  and  $> 3.5$  each containing between 23 and 49 DLA systems. P03 fitted a Schechter function,  $f(N_{\text{HI}}, z) = (f_{*}/N_{*}) (N_{\text{HI}}/N_{*})^{-\beta} \exp(-N_{\text{HI}}/N_{*})$ , to the data in each bin. Prochaska & Herbert-Fort (2004) identified six new DLA systems at  $z > 3.5$  in an automated search for DLA systems in the quasar spectra of Data Release 1 of the Sloan Digital Sky Survey (SDSS), and found that including these six new DLA systems changed the fitting parameters  $(f_{*}, N_{*}, \beta)$  of P03 significantly at  $z > 3.5$  which they

attribute to the small sample size in this bin<sup>3</sup>. For the same reason the obtained values for the fitting parameters in the lowest redshift bin are uncertain.

Not only the fitting parameters, but also the fitting function itself is uncertain. Using a Schechter function to describe  $f(N_{\text{HI}}, z)$  introduces a sharp cutoff at high  $N_{\text{HI}}$ . P03's  $f(N_{\text{HI}}, z)$  provides a good fit to the column density distribution over most of the  $z$  and  $N_{\text{HI}}$  range. However, at the high- $N_{\text{HI}}$  regime that is relevant for our purposes, other functional forms (with less sharp cut-offs in  $N_{\text{HI}}$ ) can provide equally good fits.

We therefore find that the largest uncertainties in  $f(N_{\text{HI}}, z)$  are in regions of  $(N_{\text{HI}}, z)$ -space that are most relevant for our purposes. As can be seen in Figure 1 and equation (1), the column required to produce a certain  $\tau_{0.5}$  increases rapidly with redshift ( $\propto (1+z)^{2.9}$ , for  $Z = 0.1 Z_{\odot}$ ). Because the high column systems are rare, the largest contribution to  $f_{\text{cov}}$  in the P03 model comes from low redshift. As mentioned in §2.4, 75% of the contribution to  $f_{\text{cov}}$  comes from  $z \lesssim 0.6$ .

This dominance of low redshift DLA systems is artificial since the current  $f(N_{\text{HI}}, z)$  does not capture any evolution in the number density of DLA systems in the redshift range  $z = 0 - 2$ . Observationally, it is known that the number density of DLA systems increases with redshift between  $z = 0$  and  $z = 1$  (Rao & Turnshek 2000). An improved determination of  $f(N_{\text{HI}}, z)$  that does capture the redshift evolution in the range  $z = 0 - 2$  will weaken the dominance of low redshift systems.

In summary, our estimate of  $f_{\text{cov}}$  is uncertain, but is likely to be conservative, since P03 may have underestimated the number of high  $N_{\text{HI}}$  systems, especially in the highest redshift bin. In addition, the degree to which low redshift DLA systems dominate the contribution to  $f_{\text{cov}}$  is exaggerated with the current  $f(N_{\text{HI}}, z)$ .

#### 4.3. Using X-ray Point Sources to constrain $f(N_{\text{HI}}, z)$ .

An intriguing possibility is to exploit the enhanced sensitivity to low-redshift systems to constrain  $f(N_{\text{HI}}, z)$  at low redshifts. The brightest X-ray sources Bechtold et al. (2001) have count rates of  $\sim 1 \text{ photon s}^{-1}$ ;  $\sim 3 - 15 \text{ ks}$  integrations on *Chandra* can be used to constrain whether and how much additional (to the Galaxy) absorption is present in the spectra of these sources. X-ray sources that are fainter by factor of  $\sim 10$ , which are more common, can detect a foreground DLA system with  $\tau_{0.5} = 0.1$  at the  $3\sigma$  level in 25 ksec according to equation (5) (Note that for point sources we need to multiply eq. [5] by 4, since in its derivation we assumed the X-ray was extended and binned into  $2'' \times 2''$  pixels.) The number of X-ray sources of this brightness or more is expected to be a few tens per square degree (e.g. Moretti et al. 2003). Although the redshift of the absorber is not known, with the exception of the cases in which the absorption signal is very strong (Bechtold et al. 2001), it is constrained by the redshift of the source.

It therefore seems promising to look at archival data in which sources brighter than  $0.1 \text{ counts s}^{-1}$  have been observed for 25 ks, or more generally, any archival data that has  $\gtrsim 2.5 \times 10^3 (S/3\sigma)^2$  counts from a given location and see if any additional absorption is detected at the level  $S$ . The main difficulty with this method is that the X-ray point source itself may be obscured. As a result, the amount of absorption attributed to any DLA system will be uncertain. Statistically, the distribution  $f(N_{\text{HI}}, z)$  of DLA systems could still be inferred, but would

<sup>3</sup>Prochaska & Herbert-Fort (2004) also note that P03 have obtained systematically too low values of  $N_{\text{HI}}$  for  $\log(N_{\text{HI}}/\text{cm}^{-2}) > 21$ .

require modeling of the intrinsic obscuration (e.g. Gilli et al. (2001)). A more robust approach would be to select unobscured sources, and derive upper limits on any DLA absorption, which would constrain (put upper limits) on  $f(N_{\text{HI}}, z)$ .

#### 4.4. Constraints on Galaxy Formation Scenarios

As mentioned in § 1, a spatially resolved map of the DLA gas could distinguish between the two models in which the gas resides either in a large disk, or in smaller cold clumps accreting onto to the galaxy. The large-disk models apply at  $z > 2$ , and as we saw in §2.3 the contribution to  $f_{\text{cov}}$  from  $z > 1.4$  is negligible. Although we found in §4.2 that this dominance of the lower redshift DLA systems is exaggerated, we also found in §3.1.2 that long,  $\gtrsim 3$  Ms integration times are required to detect DLA systems at  $z > 2.3$  (eq. 5). Unless future X-ray observations reveal extended X-ray sources with count rates  $> 2.5 \times 10^{-5}$  counts  $\text{s}^{-1}$ , we will not be able to detect  $z > 2.3$  DLA systems in absorption with  $\log(N_{\text{HI}}/\text{cm}^{-2}) \lesssim 22$ , which would exclude all currently known DLA systems.

We conclude that current X-ray telescopes most likely will not be able to produce maps that would enable us to distinguish between the distributions of gas predicted by the different galaxy formation scenarios. This is even more so, because the integration times mentioned above are for X-ray maps smoothed to  $2'' \times 2''$ . At  $z=2$ ,  $2''$  corresponds to  $\sim 16$  kpc, and small clumps would not be resolved. It is, however, possible to produce maps of DLA gas at  $z < 2$ . Knowledge of the  $z < 1$  systems is limited, because currently only 23 are known. For these 23 DLA systems, 14 have confirmed galaxies as counterparts, which are consistent with being drawn from a field population of galaxies (e.g. Chen 2005). For a few of these galaxies with a stellar disk, the rotation curve of the ionized gas within the stellar part of the galaxy was compared with the velocity difference between the galaxy and the DLA gas. Based on the results and the distance of the DLA gas to the center of the galaxy, it was found that the gas in the  $z < 1$  systems was consistent with being in a large disk, extending to radii larger by a factor of  $\sqrt{2}$  than those observed in local disk galaxies (see Chen 2005 and references therein). Producing maps of the DLA gas in these  $z < 1$  systems may provide an important test for this result. Increased knowledge of the  $z < 2$  systems will clearly add to the understanding of their higher redshift counterparts.

#### 5. MAPPING OUT KNOWN DLA SYSTEMS

So far we have focused on examining an extended X-ray source and searching for evidence of an intervening DLA system. As mentioned above, several hundred DLA systems are known to exist in the redshift range  $z = 0.1 - 4.6$ . A complementary approach would be to look for extended X-ray sources behind these DLA systems, and examine these extended sources for evidence of extended absorption from the DLA system.

Scharf et al. (2003) choose 4C 41.17 for X-ray study because it was an example of a cluster of submillimeter sources, centered on a powerful radio galaxy, and was therefore considered a probable proto-galaxy-cluster with X-ray emission. Extended X-ray sources at high redshifts may indeed turn out to be common, especially around radio-loud galaxies. Of the several hundred known DLA systems in front of quasars,  $\sim 10\%$  will be along sight-lines to radio-loud quasars. A certain fraction of these radio-loud quasars will be similar to 4C 41.17. This fraction is unknown at present, but is unlikely to be negligible.

The first question is, what fraction of the known DLA systems have  $\tau_{0.5} \gtrsim 0.1$ , and would therefore be good candidates for such a study. A table containing  $\sim 300$  DLA systems is given in Curran et al. (2002), for which we calculated the corresponding values of  $\tau_{0.5}$ . Since the metallicity is unknown for most of them, we assumed it to be  $0.1Z_{\odot}$ . We found a large spread in the values of  $\tau_{0.5}$ , with the maximum as high as  $\tau_{0.5} = 1.2$ . We also found that 12 and 7 DLA systems have  $\tau_{0.5} > 0.10$  and  $> 0.20$ , respectively (while this number was reduced to 8/6 when we lowered the metallicity to  $0.01Z_{\odot}$ ). The DLA systems with  $\tau_{0.5} > 0.20$  all lie at  $z < 0.7$ , and there are three at  $z > 1.4$  with  $\tau_{0.5} = 0.10 - 0.12$ . The highest value of  $\tau_{0.5} = 1.2$  is for the source detected by Bechtold et al. (2001), already mentioned above. The spectral signature is so evident in this case, that, based on the amount of X-ray absorption and the known HI column in the DLA system from its radio absorption signature, the metallicity of the DLA gas could be derived, and was found to be  $\sim 0.23Z_{\odot}$ .

The second question is: what fraction of these relatively opaque absorbers have extended X-ray emission surrounding the optical quasars in which they were discovered? An indicator for the presence of extended X-ray emission may be radio loudness (powerful radio galaxies may drive such X-ray emission, such as that found in the case of 4C 41.17). The table of DLA systems composed by Curran et al. (2002) lists the radio flux densities of the background quasars. We find that among the 12 DLA systems with  $\tau_{0.5} \gtrsim 0.1$ , at least three are in front of either a 3C or 4C source, which are radio loud. Among the other 8, at least 6 have detections in the radio. An intriguing example is Q1354+258, which is similar to 4C 41.17: it appears to have an extended structure in the radio, and is additionally known to have a diffuse Ly $\alpha$  blob around it (Heckman et al. 1991). This source would be a good first candidate to look for accompanying extended X-rays. The DLA system in front of Q1354+258 is located at  $z = 1.42$ , and it has a column of  $3.2 \times 10^{21} \text{ cm}^{-2}$  (e.g., Rao & Turnshek 2000). Note that the metallicity of this DLA system is  $Z \sim 0.02Z_{\odot}$  (Vladilo 2002) instead of  $Z = 0.1Z_{\odot}$  which slightly lowers  $\tau_{0.5}$  from 0.12 to 0.09. This implies that if extended X-rays are detected from Q1354+258, it should be brighter than 4C 41.17 for a detection at the  $S = 2 - \sigma$  level in  $\lesssim 3$  Ms on *Chandra*.

The above exploratory remarks suggest that a full systematic search for DLA systems, whose parent quasars are similar to 4C 41.17, and deep X-ray observations of these sources, is a promising alternative approach to discover X-ray silhouettes of DLA systems.

#### 6. CONCLUSIONS

The neutral hydrogen column densities in observed DLA systems are in the range  $\log(N_{\text{HI}}/\text{cm}^{-2}) = 20 - 21.7$  (e.g. Curran et al. 2002) and are high enough to absorb a measurable fraction of soft X-ray photons from a background source. We defined the parameter  $\tau_{0.5}$ , which is the optical depth through DLA systems for a photon with an observed energy of 0.5 keV. We showed in §2.3 that  $\sim 1\%$  of the sky is covered by DLA systems which have  $\tau_{0.5} \geq 0.2$  when the background X-ray sources lie at redshifts  $z \gtrsim 1.4$ . This result depends on the assumed column density distribution  $f(N_{\text{HI}}, z)$ , which is at present poorly constrained, and also on the mean metallicity of the DLA systems, which we assumed to be  $Z = 0.1Z_{\odot}$  based on the observed value (e.g. Prochaska et al. 2003). We discussed uncertainties in  $f_{\text{cov}}$  in §2.4 and found that the values we found are most

likely conservative.

An optical depth of  $\tau_{0.5} = 0.2$  will introduce a dimming in the soft X-ray bands by  $\sim 20\%$ , an amount that is much lower than intrinsic brightness fluctuations. However, as we discussed in §3, absorption by an intervening DLA system can be distinguished from intrinsic brightness fluctuations by looking for the spectral signatures of absorption (§3.1, Fig. 3) and/or combining the X-ray observations with an SZ decrement map of the area (§3.2). We showed in §3.1.1 that in order to reliably detect a DLA absorption signature on top of the spectral imprint left by Galactic HI,  $\gtrsim 300$  photons per angular resolution element are required in the 0.3–8 keV band to detect a DLA system with  $\tau_{0.5} = 0.2$  at the  $2\sigma$  level.

For diffuse, high redshift X-ray sources similar to 4C 41.17 (Scharf et al. 2003) and 3C 294 (Fabian et al. 2003), this requires observation times of a few megaseconds on *Chandra* when the maps are smoothed to  $\sim 2''$  resolution. The influence of the brightness of the background X-ray source, the slope of the X-ray spectrum and the value of  $\tau_{0.5}$  on the required integration time on *Chandra* are detailed in §3.1.2.

We discuss the implications of the poor constraints on the absorber’s redshift using this method in §4.1 and find two possible contaminants that cannot be ruled out observationally. These are (1) neutral hydrogen physically associated with the X-ray source and (2) a small, compact nearby HI cloud. Both are astrophysically interesting as we argued in §4.1. We suggested a new method to use archival data of bright (count rates  $> 0.1$  photons  $s^{-1}$ ) X-ray point sources to constrain the poorly known low-redshift column density distribution function,  $f(N_{\text{HI}}, z)$ , in §4.3.

The inverse method is discussed in §5 in which we presented the possibilities of mapping out known DLA systems using an X-ray background source. We found that out of the sample of  $\sim 300$  DLA systems tabulated in Curran et al. (2002), 12 have  $\tau_{0.5} > 0.1$ , with values anywhere in the range  $\tau_{0.5} = 0.1 – 1.2$ . We found that at least 4 of these sources resemble 4C 41.17 and 3C 294 in their radio loudness and at least one of them also has a surrounding extended Ly $\alpha$  halo. These 4 sources are promising candidates to have extended X-ray emission associated with them, and, if such X-ray emission is revealed in deep X-ray follow-ups, they would be suitable to search for DLA silhouettes.

Although challenging, X-ray silhouettes are likely to be the only viable method to directly spatially resolve hydrogen gas in distant DLA systems in the foreseeable future. Among planned future radio telescopes, only SKA will be able to detect 21cm emission from neutral hydrogen at  $z > 0.5$  (e.g., van der Hulst et al. 2004), and extended Ly $\alpha$  emission would only be detectable for DLAs in the immediate vicinity of a luminous ionizing source.

The planned X-ray observatories, *the X-ray Evolving Universe Spectrometer* (XEUS; Parmar et al. 2003) and *Generation X* (Zhang et al. 2002) are expected to have  $\sim 0.1'' – 1''$  resolution, and a sensitivity of 1 or 2 orders of magnitude better than *Chandra*, extending to energies as low as 0.1 keV. At these low energies, absorption by a foreground DLA system will leave a much stronger imprint. The X-ray silhouettes of DLA systems should be feasible to detect in routine observations with these planned instruments.

We thank Joop Schaye, Jason Prochaska and Art Wolfe for useful comments. We thank the referee, Ariyeh Maller, for

constructive comments that significantly improved the presentation of this paper. ZH gratefully acknowledges support by the National Science Foundation through grants AST-0307291 and AST-0307200 and by NASA through grants HST-GO-09793.18 and NNG04GI88G. CS acknowledges the support of NASA/*Chandra* grant SAO G03-4158A.

## REFERENCES

Bagla, J. S. 1999, in ASP Conf. Ser. 156: Highly Redshifted Radio Lines, 9–15  
 Bahcall, J. N., & Peebles, P. J. E. 1969, ApJ, 156, L7+  
 Bechtold, J., Siemiginowska, A., Aldcroft, T. L., Elvis, M., & Dobrzycki, A. 2001, ApJ, 562, 133  
 Birnboim, Y., & Dekel, A. 2003, MNRAS, 345, 349  
 Briggs, F. H., Wolfe, A. M., Liszt, H. S., Davis, M. M., & Turner, K. L. 1989, ApJ, 341, 650  
 Chen, H., & Lanzetta, K. M. 2003, ApJ, 597, 706  
 Chen, H.-W. 2005, in ASP Conf. Ser. 331, Extra-planar Gas Conference, astro-ph/0410558, ed. R. Braun  
 Clarke, T. E., Uson, J. M., Sarazin, C. L., & Blanton, E. L. 2004, ApJ, 601, 798  
 Curran, S. J., Webb, J. K., Murphy, M. T., Bandiera, R., Corbelli, E., & Flambaum, V. V. 2002, Publications of the Astronomical Society of Australia, 19, 455  
 Fabian, A. C., Sanders, J. S., Crawford, C. S., & Ettori, S. 2003, MNRAS, 341, 729  
 Fynbo, J. U., Møller, P., & Warren, S. J. 1999, MNRAS, 305, 849  
 Gilli, R., Salvati, M., & Hasinger, G. 2001, A&A, 366, 407  
 Grego, L., Vrtilek, J. M., Van Speybroeck, L., David, L. P., Forman, W., Carlstrom, J. E., Reese, E. D., & Joy, M. K. 2004, ApJ, 608, 731  
 Hachnelt, M. G., Steinmetz, M., & Rauch, M. 1998, ApJ, 495, 647  
 Heckman, T. M., Miley, G. K., Lehnert, M. D., & van Breugel, W. 1991, ApJ, 370, 78  
 Kanekar, N., & Briggs, F. H. 2003, A&A, 412, L29  
 Katz, N., Weinberg, D. H., & Hernquist, L. 1996, ApJS, 105, 19  
 Keres, D., Katz, N., Weinberg, D. H., & Dave, R. 2004, MNRAS, submitted  
 Kocsis, B., Haiman, Z., & Frei, Z. 2005, ApJ, in press, astro-ph/0409430  
 Lockman, F. J. 2003, in Soft X-ray Emission from Clusters of Galaxies and Related Phenomena, astro-ph/0311386, ed. R. Lieu & J. Mittaz  
 Lockman, F. J., & Pidopryhora, Y. 2004, in Proceedings of the Extra-planar Gas Conference, astro-ph/0410161, ed. R. Braun  
 Maller, A. H., Prochaska, J. X., Somerville, R. S., & Primack, J. R. 2001, MNRAS, 326, 1475  
 —. 2003, MNRAS, 343, 268  
 Moretti, A., Campana, S., Lazzati, D., & Tagliaferri, G. 2003, ApJ, 588, 696  
 Péroux, C., McMahon, R. G., Storrie-Lombardi, L. J., & Irwin, M. J. 2003, MNRAS, 346, 1103  
 Parmar, A. N., Hasinger, G., Arnaud, M., Barcons, X., Barret, D., Blanchard, A., Boehringer, H., Cappi, M., Comastri, A., Courvoisier, T., Fabian, A. C., Georgantopoulos, I., Griffiths, R., Kawai, N., Koyama, K., Makishima, K., Malaguti, P., Mason, K. O., Mutch, C., Mendez, M., Ohashi, T., Paerels, F., Piro, L., Schmitt, J., van der Klis, M., & Ward, M. 2003, in X-Ray and Gamma-Ray Telescopes and Instruments for Astronomy. Edited by Joachim E. Truemper, Harvey D. Tananbaum. Proceedings of the SPIE, Volume 4851, pp. 304–313 (2003)., 304–313  
 Prochaska, J. X., Gawiser, E., Wolfe, A. M., Castro, S., & Djorgovski, S. G. 2003, ApJ, 595, L9  
 Prochaska, J. X., & Herbert-Fort, S. 2004, PASP, 116, 622  
 Prochaska, J. X., & Wolfe, A. M. 1997, ApJ, 487, 73  
 Rao, S. M., Nestor, D. B., Turnshek, D. A., Lane, W. M., Monier, E. M., & Bergeron, J. 2003, ApJ, 595, 94  
 Rao, S. M., & Turnshek, D. A. 2000, ApJS, 130, 1  
 Raymond, J. C., & Smith, B. W. 1977, ApJS, 35, 419  
 Scharf, C., Smail, I., Ivison, R., Bower, R., van Breugel, W., & Reuland, M. 2003, ApJ, 596, 105  
 Siemiginowska, A., Bechtold, J., Aldcroft, T. L., Elvis, M., Harris, D. E., & Dobrzycki, A. 2002, ApJ, 570, 543  
 Spergel, D. N., Verde, L., Peiris, H. V., Komatsu, E., Nolta, M. R., Bennett, C. L., Halpern, M., Hinshaw, G., Jarosik, N., Kogut, A., Limon, M., Meyer, S. S., Page, L., Tucker, G. S., Weiland, J. L., Wollack, E., & Wright, E. L. 2003, ApJS, 148, 175  
 Storrie-Lombardi, L. J., & Wolfe, A. M. 2000, ApJ, 543, 552  
 van der Hulst, J. M., Sadler, E. M., Jackson, C. A., Hunt, L. K., Verheijen, J. H., & van Gorkom, J. H. 2004, in Science with the Square Kilometer Array, ed. C. Carilli & S. Rawlings (Elsevier Science Publishers)  
 Vladilo, G. 2002, A&A, 391, 407  
 Wakker, B. P., & van Woerden, H. 1997, ARA&A, 35, 217  
 Wilms, J., Allen, A., & McCray, R. 2000, ApJ, 542, 914  
 Wolfe, A. M., Lanzetta, K. M., Foltz, C. B., & Chaffee, F. H. 1995, ApJ, 454, 698  
 Zhang, W., Petre, R., & White, N. 2002, in COSPAR, Plenary Meeting